Chemical Communications

Electronic Supporting Information for:

Sterically controlled self-assembly of tetrahedral M_6L_4 cages via cationic N-donor ligands

Anssi Peuronen,[a] Samu Forsblom[a] and Manu Lahtinen[a]*

[a]*Department of Chemistry, University of Jyväskylä, P.O. Box 35, Jyväskylä, FI-40014-JY, Finland.*

*manu.k.lahtinen@jyu.fi

Table of Contents

Experimental details

All starting materials were purchased from Sigma-Aldrich and were used without further purification. Ligands 1,3,5-tris(DABCO-N-methyl)benzene tri(hexafluorophosphate) (**L1**) and 2,4,6-tris(DABCO-N-methyl)mesitylene tri(hexafluorophosphate) (**L2**), were synthesized following the procedure described by Garratt et al.[1] Bis(trifluoromethylsulfonyl)imide (NTf_2^-) salt of **L2** [**L2**$(NTf_2^-)_3$] was prepared similarly to PF_6^- salt by a method described by Garratt et al. using lithium bis(trifluoromethylsulfonyl)imide instead of NH_4PF_6.

Self-assembly reactions were carried out at ambient conditions in 5 ml glass vials using HPLC grade acetonitrile with 6:4 metal-ligand ratios. Change in the metal-ligand stoichiometry did not affect the composition of the cage. Single crystals of **1-3** were grown by dissolving $Cu(OTf)_2$ and corresponding ligand (in 6:4 ratio) into 1-2 ml of acetonitrile (4-5 ml for **2**, in order to completely dissolve the sample) and allowing the solution to evaporate slowly (see Fig. S1 for pictures of the crystals). Respective bulk samples of **1** and **2** were prepared similarly except a stoichiometric amount of KPF_6 was added to the reaction mixture in order to improve the yield. In case of compound **1**, diethyl ether was used to afford a precipitate whereas compound **2** precipitated out immediately after mixing **L2** with $Cu(OTf)_2$. The obtained precipitates were separated by decantation and dried in air prior to elemental analyses (Vario EL III). All samples lose most of the solvent molecules after they are removed from their mother liquor.

Compound **1**: 20 μmol (17.8 mg) of **L1**$(PF_6)_3$ and a mixture of 30 μmol (10.9 mg) of $Cu(OTf)_2$ and 60 μmol (11.1 mg) of KPF_6 were dissolved separately in 0.5 ml of acetonitrile. Mixing the two solutions gave a green solution from which the product was precipitated by a slow addition of diethyl ether. The precipitate was separated by decantation and dried in air. Yield 19.2 mg, (3.2 μmol for Cu_6(**L1**$)_4(PF_6)_{24}\cdot(CH_3CN)_8$), 66 %, based on Cu. Anal.calcd. (%) C, 24.81; H, 3.42; N, 7.47. Found (%): C, 24.74; H, 3.45; N, 7.61.

Compound **2**: 20 μmol (18.6 mg) of **L2**$(PF_6)_3$ and a mixture of 30 μmol (10.9 mg) of $Cu(OTf)_2$ and 60 μmol (11.1 mg) of KPF_6 were dissolved separately in 0.5 ml of acetonitrile. Mixing the two solutions led to a quick precipitation of the product as a green solid which was washed with small amount of MeCN, separated by decantation and dried in air. Yield 14.6 mg, (2.4 μmol for Cu_6(**L2**$)_4(PF_6)_{24}\cdot(CH_3CN)_3$), 49 %, based on Cu. Anal.calcd. (%) C, 25.36; H, 3.60; N, 6.34. Found (%): C, 25.51; H, 3.66; N, 6.32.

Compound **3**: 13 μmol (17.8 mg) of **L2**$(NTf_2)_3$ and 20 μmol (7.3 mg) of $Cu(OTf)_2$ were dissolved separately into 0.5 ml of acetonitrile. Mixing the two solutions gave a green/yellowish solution which was left to evaporate slowly. After two days, a small batch of single crystals of **3** was separated and dried in air. Yield 3.5 mg, (0.45 μmol for $(Cu(H_2O))_6$(**L2**$)_4(CF_3SO_3)_{12}((CF_3SO_2)_2N)_{12}\cdot(CH_3CN)_3$), 14 %, based on Cu. Anion composition was deduced from the single crystal structure. Anal.calcd. (%) C, 25.12; H, 2.93; N, 7.05. Found (%): C, 25.21; H, 3.01; N, 7.36.

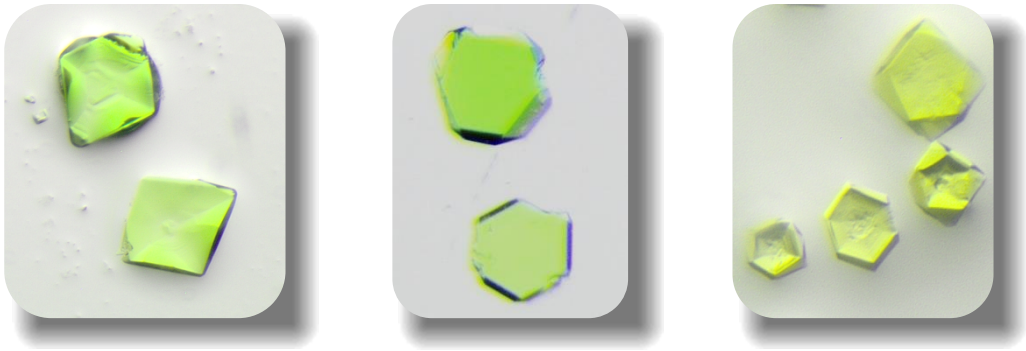

Fig. S1. Pictures of crystal of compounds **1** (left), **2** (middle) and **3** (right). Average crystal sizes vary between 100 and 300 µm.

^{1}H and ^{19}F NMR studies

Tetrakis(acetonitrile)palladium(II) tetrafluoroborate ($Pd(BF_4)_2$) was used to study the self-assembly of M_6L_4 species with **L1** and **L2** in solution. These reactions were carried out by mixing 10 µmol of $Pd(BF_4)_2$ and 6.7 µmol of **L1** and **L2**, respectively, in 0.6 ml of CD_3CN. The respective ^{1}H NMR spectra, recorded with Bruker Avance 300 spectrometer, show quantitative formation of Pd_6(**L1**)$_4$ and Pd_6(**L2**)$_4$ species in solution: ^{1}H NMR (300 MHz, 300 K), Pd_6(**L1**)$_4$: δ = 3.61 (s, 36H; N-CH_2-CH_2-N), 4.53 (s, 6H; N-CH_2-Ar), 7.69 (s, 3H; H-Ar); Pd_6(**L2**)$_4$: δ = 2.55 (s, 9H; -CH_3), 3.63 (s, 36H; N-CH_2-CH_2-N), 4.80 (s, 6H; N-CH_2-Ar).

We also investigated the solution state anion binding by monitoring the ^{19}F NMR shifts of PF_6^- and BF_4^- anions while cooling the samples from room temperature to 238 K. There was however no indication of encapsulation of either of the two anions by NMR (Fig. S2). This is probably due to the rapid exchange of anions from exo- to endohedral surrounding in solution. ^{19}F NMR (282.4 MHz, 300 K), Pd_6(**L2**)$_4$: δ = -153.86 (s; $^{11}BF_4^-$), δ = -153.81 (s; $^{10}BF_4^-$) (total of 12 BF_4^-), δ = -75.33 (d, ^{1}J = 708 Hz; 12PF_6^-). Aqueous KF (-125.3 ppm) was used as an external standard.

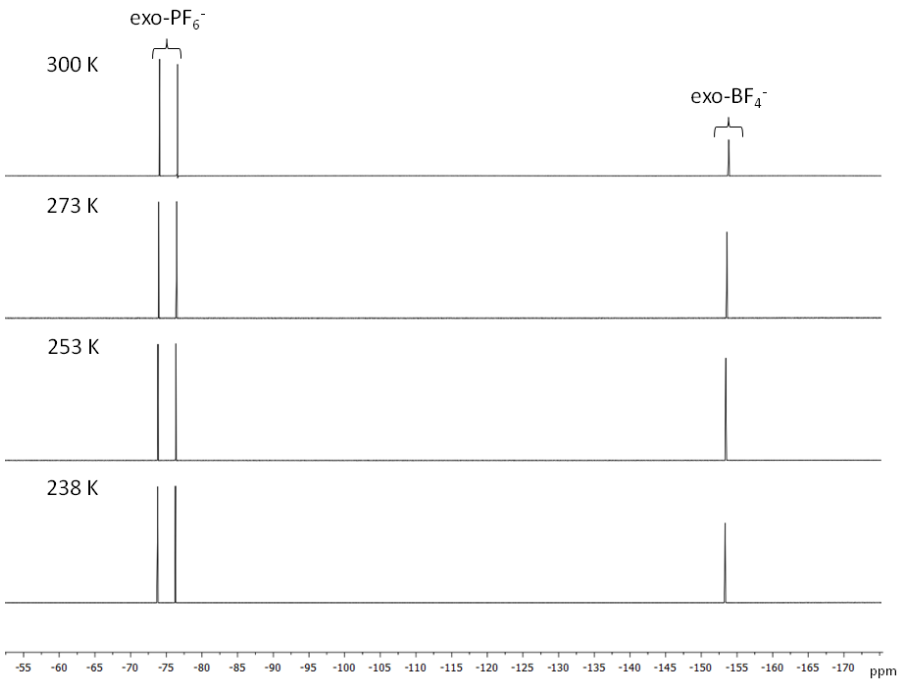

Fig. S2. ^{19}F NMR spectrum of $Pd_6(\mathbf{L2})_4(BF_4)_{12}(PF_6)_{12}$ measured in CD_3CN at various temperatures.

Single crystal X-ray measurements

All single crystal X-ray data were collected with Agilent SuperNova, equipped with multilayer optics monochromated dual source (Cu and Mo) and Atlas detector, using Cu Kα (1.54184 Å) radiation at temperature 123 K (Table S1). Data acquisitions, reductions and analytical face-index based absorption corrections were made using program CrysAlisPRO.[2] The structures were solved with either ShelXS[3] or Superflip[4] programs and refined on F^2 by full matrix least squares techniques with ShelXL[3] program in Olex[2] (v.1.2) program package.[5] Anisotropical displacement parameters were applied for all atoms except hydrogens which were calculated into their ideal positions using isotropic displacement parameters 1.2-1.5 times of the host atom. Solvent mask, as implemented in Olex[2] (similar to PLATON/SQUEEZE), was used to treat the unresolved electron density corresponding to disordered anions and solvent molecules in the crystal lattices. For **1**, 1902 electrons (void of 4684 Å^3) per unit cell were treated with solvent masking, corresponding to 40 MeCN molecules and 16 PF_6^- anions. In case of **2**, in which the main part of disorder arises from the two-fold symmetry-imposed disorder of the cage assembly which partially overlaps with some of the solvent atoms, a total of 1264 electrons (void of 5374 Å^3) per unit cell corresponding to 56 MeCN molecules and 16 PF_6^- were treated. The exohedral environment in structure **3** (9551 Å^3 and 6539 electrons / unit cell) is severely disordered and could not be resolved from the residual electron density. We deduced the most probable anion composition as 12 OTf^- and 12 NTf_2^- anions per cage (including the four encapsulated OTf^-) which also agrees with the results of elemental analysis. Consequently, 16 OTf- and 24 NTf_2^- anions were omitted from the data together with 10 MeCN molecules which occupy the remaining space in the lattice.

Details of refinement of structure 2: In crystal structure of **2**, all atoms, except two of the CH_2-groups, lie in special positions of the asymmetric unit. When the site specific symmetry operations are applied to all atoms a caged structure is generated where each Cu(II) is coordinated to four distinct ligands. This would mean a formation of an octahedral $Cu_6(\mathbf{L2})_8$ species. Close inspection of the structure reveals suspiciously short inter-ligand distances around the Cu(II) coordination environment [d(C1···C1′) = 2.002(19) Å, d(H1A···H1A′) = 0.384(1) Å; (′) = (x, y, -z)]. A better agreement of the overall R-value in the structure

refinement is achieved by halving the site occupancy of atoms belonging to the ligand. In so doing, Cu-coordinated MeCN, disordered together with the ligand, can be identified from the electron density map. Hence, **2** is best described by two tetrahedral Cu_6(**L2**)$_4$ cages disordered in 0.5:0.5 ratio.

Details of refinement of structure 3: Compound **3** crystallizes in non-centrosymmetric cubic space group *I*-43*m*. As in **2**, the asymmetric unit consists of 1/24 of the Cu_6(**L2**)$_4$ cage and OTf^- anion (Z' = 0.04167). The endohedral coordination environment of the Cu-atom deviates from the ones found in structures **1** and **2** as only a single endohedral Q-peak is found within 2.36 Å of the Cu-atom. Best fit was achieved by refining an oxygen atom to this position corresponding to a Cu-coordinated water molecule. Statistical analysis of representative crystal structures in Cambridge Crystallographic Database also show similar Cu-O distances between H_2O and Cu. Furthermore, a good agreement between measured and calculated CHN values is reached when the water molecules are taken into account.

Table S1. Crystallographic data for structures of **1-3**.

	1	**2**	**3**
Empirical formula	$C_{208}H_{330}N_{74}F_{144}P_{24}Cu_6$	$C_{208}H_{336}N_{68}F_{144}P_{24}Cu_6$	$C_{190}H_{267}N_{53}F_{108}O_{90}S_{36}Cu_6$
Formula weight	7727.96	7649.95	8320.95
Temperature/K	123.0(1)	123.0(1)	123.0(1)
Crystal system	tetragonal	cubic	cubic
Space group	$P4_2/nnm$	Fm-3m	I-43m
a/Å	22.4999(5)	31.8441(2)	25.2831(2)
b/Å	22.4999(5)	31.8441(2)	25.2831(2)
c/Å	31.3098(12)	31.8441(2)	25.2831(2)
α/°	90	90	90
β/°	90	90	90
γ/°	90	90	90
Volume/Å^3	15850.4(9)	32291.5(7)	16161.8(4)
Z	2	4	2
ρ_{calc}mg/mm^3	1.619	1.574	1.71
m/mm^{-1}	2.894	2.828	3.951
F(000)	7852	15560	8440
Crystal size/mm^3	0.153 × 0.069 × 0.054	0.176 × 0.148 × 0.036	0.147 × 0.114 × 0.050
Radiation	CuKα (λ = 1.54184)	CuKα (λ = 1.54184)	CuKα (λ = 1.54184)
2Θ range for data collection	6.232 to 133.972°	7.852 to 133.838°	8.566 to 124.448°
Index ranges	$-26 \le h \le 20$, $-19 \le k \le 27$, $-38 \le l \le 33$	$-27 \le h \le 38$, $-27 \le k \le 37$, $-16 \le l \le 25$	$-6 \le h \le 20$, $-5 \le k \le 28$, $-27 \le l \le 18$
Reflections collected	45580	13856	5126
Independent reflections	7301 [R_{int} = 0.1033, R_{sigma} = 0.0476]	1474 [R_{int} = 0.0259, R_{sigma} = 0.0113]	1889 [R_{int} = 0.0251, R_{sigma} = 0.0243]
Data/restraints/ parameters	7301/60/496	1474/169/196	1889/71/114
Goodness-of-fit on F^2	1.021	1.842	0.994
Final R indexes [I>=2σ (I)]	R_1 = 0.0939, wR_2 = 0.2699	R_1 = 0.1338, wR_2 = 0.3689	R_1 = 0.0564, wR_2 = 0.1542
Final R indexes [all data]	R_1 = 0.1186, wR_2 = 0.2989	R_1 = 0.1413, wR_2 = 0.3827	R_1 = 0.0638, wR_2 = 0.1632
Largest diff. peak/hole / e Å^{-3}	0.61/-0.59	1.50/-1.47	0.37/-0.27
Flack parameter			0.10(5)

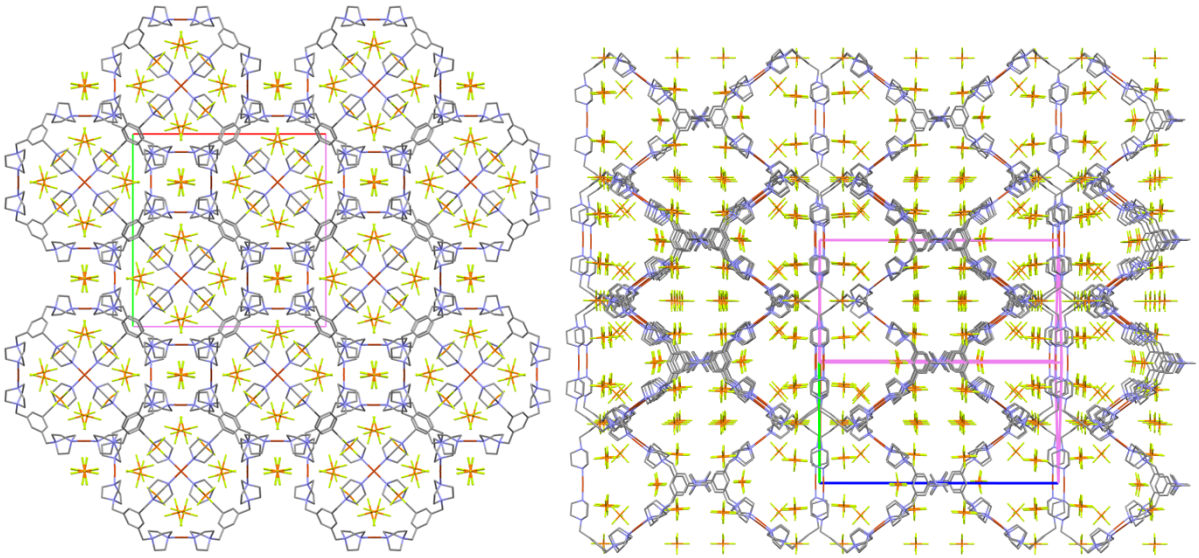

Fig. S3. Packing schemes of structure **1** viewed along crystallographic *c*-axis (left) and (110) lattice plane (right). Hydrogen atoms and solvent molecules are omitted from the figure. Atom colors (in figures S3-S6): C, grey; N, blue; F, green; P, orange; Cu, brown.

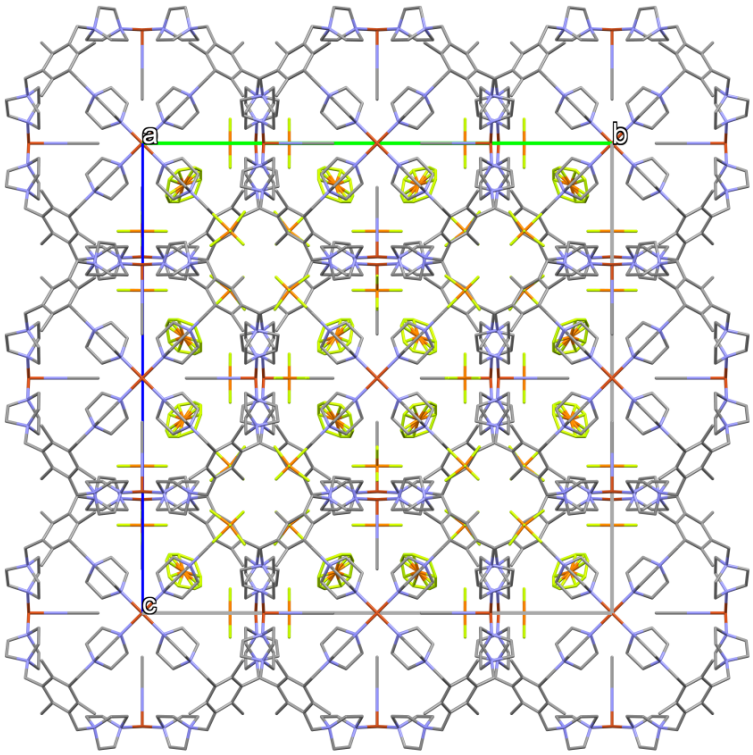

Fig. S4. Packing scheme of structure **2** viewed along crystallographic *a*-axis. Hydrogen atoms and solvent molecules are omitted from the figure.

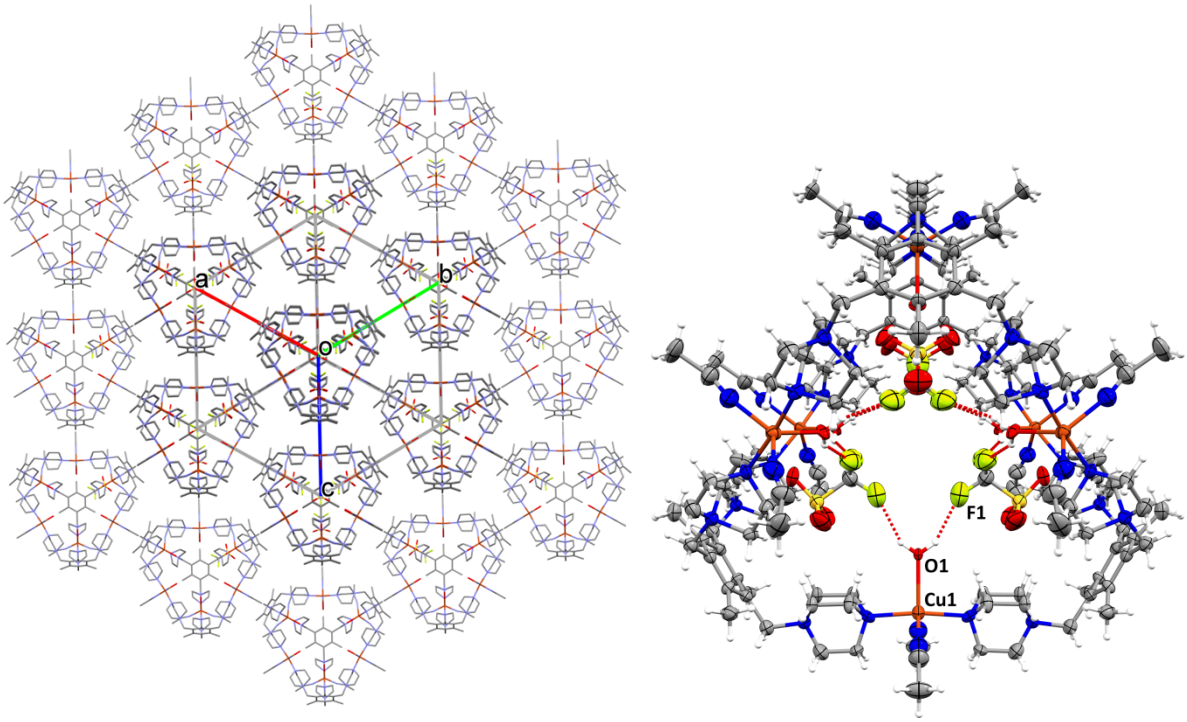

Fig. S5. Left: packing scheme of structure **3** viewed along the diagonal of the unit cell. Right: detailed view of the endohedral environment of structure **3**. Distances (Å): Cu1-O1 = 2.363(5), O1···F1 = 2.934(12) Å. Ellipsoids are drawn at the 20 % probability level.

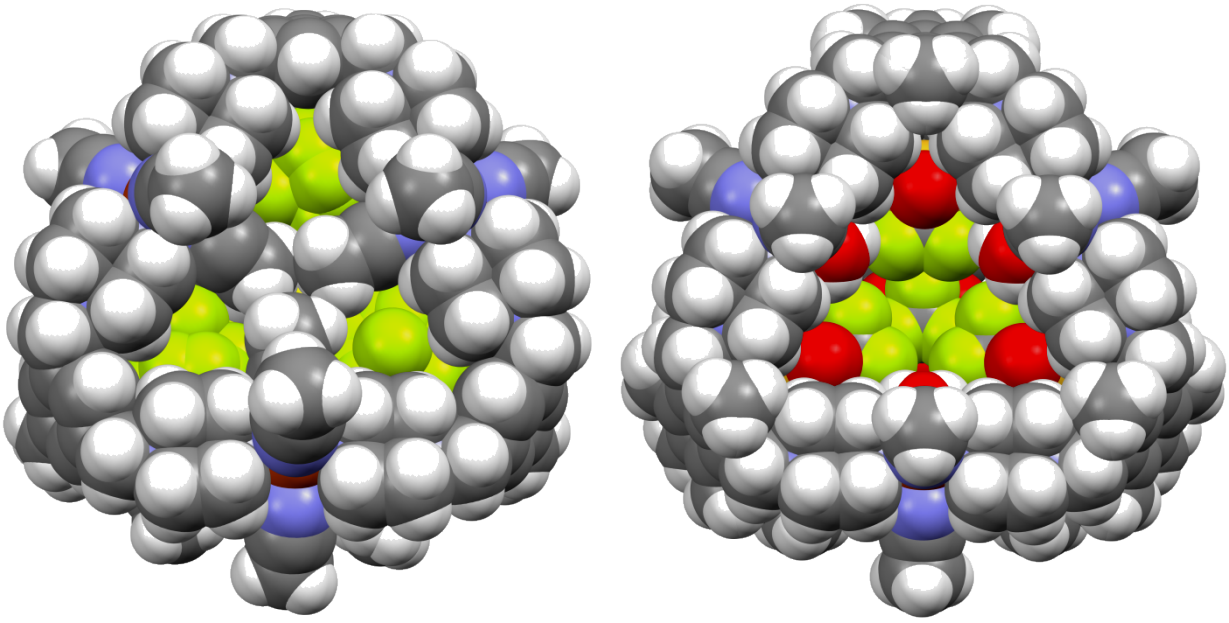

Fig. S6. Space-filling models of cages Cu_6**(L1)**$_4$ (left) and Cu_6**(L2)**$_4$ (right) in **1** and **3**, respectively.

Computational details

In order to estimate the effect of mono-alkylation of DABCO to its capability to act as an nucleophile toward *d*-block elements, we conducted a brief computational analysis of copper(I)chloride complex N-methylated DABCO (complex **I**), made charge neutral by adding a chloride counterion, and compared it with its neutral counterpart (complex **II**). Furthermore, these results were compared with corresponding pyridine complex (complex **III**) in order to evaluate the difference in bonding strength of the new introduced ligand species to a more commonly used coordinating group.

Geometries of the three complexes (Fig. S7, Table S3) were optimized with Gaussian 09[6] using DFT (PBEPBE functional[7]) with high quality triple-ζ basis sets (def2-TZVPP) and the subsequent geometries were verified as minima in the potential energy surface by vibrational analysis. We then evaluated the bonding interactions between the metal and ligand using energy decomposition analysis (EDA) as implemented in the program ADF 2012.1 (Table S2).[8] This method allows the decomposition of interaction energy (ΔE_{int}) between preselected (non-relaxed) fragments into three terms: Pauli repulsion (ΔE_{Pauli}), electrostatic interaction (ΔE_{elstat}) and orbital interaction (ΔE_{orb}). The ΔE_{orb} term can be furthermore broken down according to irreducible representations of the molecular point group. ΔE_{Pauli} is the source of destabilizing interactions between the molecular fragments whereas ΔE_{elstat} and ΔE_{orb} are both stabilizing.

The optimized geometries of **I** and **II** show only minor differences in regards to metal-ligand distances (Fig. S7). In respect of total bonding interactions (ΔE_{int}) the mono-alkylation of DABCO weakens the bond between the metal and ligand by roughly 25 kJ/mol (13 %) (Table S2). The main contribution to the difference in bonding between **I** and **II** arises from ΔE_{elstat} (ca. 30 kJ/mol, 8 %) whereas ΔE_{Pauli} and ΔE_{orb} exhibit substantially smaller changes (3 % each). Thus according to EDA, the mono-alkylation of DABCO weakens the electrostatic interaction (ΔE_{elstat}) of the metal-ligand bond, whereas the covalent character of the bond (ΔE_{orb}) remains virtually unchanged. ΔE_{int} value of -201.5 kJ/mol for the metal-ligand bond in **III** means that, according to our simplified model, a single Cu-pyridine bond is roughly 20% stronger compared to mono-alkylated DABCO.

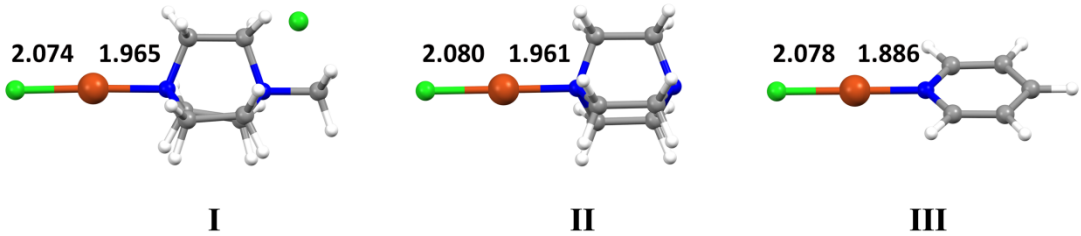

Fig. S7. Optimized geometries of copper(I)chloride complexes of N-methyl-DABCO chloride (**I**), DABCO (**II**) and pyridine (**III**). Distances are reported in Ångströms. Color coding: Cu (brown), Cl (green), N (blue), C (grey) and H (white).

Table S2. Results of energy decomposition analysis (PBE/TZ2P).

	I	II	III
ΔE_{pauli}	289.7	298.4	336.9
ΔE_{elstat}	-324.5	-353.8	-384.9
ΔE_{orb}	-127.3	-131.4	-153.6
ΔE_{int}	-162.2	-186.8	-201.5

Table S3. xyz-coordinates and electronic energies (in parenthesis in Hartrees) for optimized structures of complexes **I**, **II** and **III**.

I (-2945.29255369)				**II** (-2445.41247462)				**III** (-2348.47322811)			
C	-0.45456	-0.00202	-1.55700	C	0.68496	1.18638	1.16611	Cu	-0.00043	-2.79645	0.00000
N	-0.07455	-0.95511	-0.48494	N	0.00000	0.00000	1.65747	Cl	-0.00075	-4.87473	0.00000
C	-1.02811	-0.78969	0.66245	C	0.68496	-1.18638	1.16611	N	-0.00014	-0.91077	0.00000
C	-1.08788	0.69108	1.04967	C	0.69498	-1.20374	-0.38028	C	-1.16106	-0.21032	0.00000
N	0.01349	1.43881	0.40619	N	0.00000	0.00000	-0.89664	C	-1.19834	1.17900	0.00000
C	-0.20356	1.42907	-1.05316	C	0.69498	1.20374	-0.38028	C	0.00029	1.89333	0.00000
C	1.27618	0.72264	0.70105	C	-1.38995	0.00000	-0.38028	C	1.19871	1.17863	0.00000
C	1.31525	-0.61993	-0.02463	C	-1.36992	0.00000	1.16611	C	1.16099	-0.21068	0.00000
C	-0.10858	-2.36441	-0.94874	Cu	0.00000	0.00000	-2.85774	H	-2.07535	-0.80269	0.00000
Cu	0.06759	3.30144	1.03093	Cl	0.00000	0.00000	-4.93759	H	-2.16177	1.68759	0.00000
Cl	0.09295	5.29761	1.59257	H	0.18471	-2.07893	-0.78454	H	0.00046	2.98343	0.00000
H	-0.98988	0.79590	2.12917	H	1.70805	-1.19943	-0.78454	H	2.16229	1.68693	0.00000
H	-2.02679	1.15889	0.75191	H	1.70186	-1.18791	1.56405	H	2.07511	-0.80333	0.00000
H	-1.99406	-1.16422	0.32469	H	0.17783	-2.06781	1.56405				
H	-0.62854	-1.44023	1.45850	H	-1.89276	-0.87951	-0.78454				
H	1.32648	0.56520	1.77867	H	-1.89276	0.87951	-0.78454				
H	2.11714	1.34892	0.40689	H	-1.87969	-0.87990	1.56405				
H	1.60978	-1.43045	0.66146	H	-1.87969	0.87990	1.56405				
H	1.93603	-0.60247	-0.92125	H	1.70805	1.19943	-0.78454				
H	-1.05203	2.06992	-1.28844	H	0.18471	2.07893	-0.78454				
H	0.67778	1.86386	-1.52331	H	0.17783	2.06781	1.56405				
H	0.14190	-0.23128	-2.43959	H	1.70186	1.18791	1.56405				
H	-1.50414	-0.18132	-1.79129								
H	0.15069	-2.98456	-0.08132								
H	0.62269	-2.48276	-1.74701								
H	-1.10903	-2.58547	-1.31781								
Cl	0.91377	-2.84942	2.22435								

References

1 P. J. Garratt, A. J. Ibbett, J. E. Ladbury, R. O'Brien, M. B. Hursthouse and K. M. Abdul Malik, *Tetrahedron,* 1998*,* **54***,* 949–968.

2 CrysAlis^{Pro} program, version 1.171.36.21, Agilent Technologies, Oxford, 2012.

3 G.M. Sheldrick, *Acta Crystallogr.* 2008, **A64**, 112–122.

4 L. Palatinus and G. Chapuis, *J. Appl. Cryst.* 2007, **40**, 786–790.

5 O. V. Dolomanov, L. J. Bourhis, R. J. Gildea, J. A. K. Howard and H. J. Puschmann, *Appl. Cryst.*, 2009, **42**, 339–341.

6 Gaussian 09, Revision C.01, M. J. Frisch, G. W. Trucks, H. B. Schlegel, G. E. Scuseria, M. A. Robb, J. R. Cheeseman, G. Scalmani, V. Barone, B. Mennucci, G. A. Petersson, H. Nakatsuji, M. Caricato, X. Li, H. P. Hratchian, A. F. Izmaylov, J. Bloino, G. Zheng, J. L. Sonnenberg, M. Hada, M. Ehara, K. Toyota, R. Fukuda, J. Hasegawa, M. Ishida, T. Nakajima, Y. Honda, O. Kitao, H. Nakai, T. Vreven, J. A. Montgomery, Jr., J. E. Peralta, F. Ogliaro, M. Bearpark, J. J. Heyd, E. Brothers, K. N. Kudin, V. N. Staroverov, R. Kobayashi, J. Normand, K. Raghavachari, A. Rendell, J. C. Burant, S. S. Iyengar, J. Tomasi, M. Cossi, N. Rega, J. M. Millam, M. Klene, J. E. Knox, J. B. Cross, V. Bakken, C. Adamo, J. Jaramillo, R. Gomperts, R. E. Stratmann, O. Yazyev, A. J. Austin, R. Cammi, C. Pomelli, J. W. Ochterski, R. L. Martin, K. Morokuma, V. G. Zakrzewski, G. A. Voth, P. Salvador, J. J. Dannenberg, S. Dapprich, A. D. Daniels, Ö. Farkas, J. B. Foresman, J. V. Ortiz, J. Cioslowski and D. J. Fox, Gaussian, Inc., Wallingford CT, 2009.

7 J. P. Perdew, K. Burke and M. Ernzerhof, *Phys. Rev. Lett.*, 1996, **77**, 3865-3868.

8 G. te Velde, F.M. Bickelhaupt, S.J.A. van Gisbergen, C. Fonseca Guerra, E.J. Baerends, J.G. Snijders and T. Ziegler, *J. Comput. Chem.* 2001, **22**, 931–967.